Femtosecond laser welded nanostructures and plasmonic devices

A. Hu, P. Peng, and H. Alarifi
Department of Mechanical and Mechatronics Engineering, Centre for Advanced Material Joining, University of Waterloo, 200 University Ave. West, Waterloo, Ontario N2L 3G1, Canada

X. Y. Zhang and J. Y. Guo
School of Electronic Science and Engineering, Southeast University, Nanjing 210096, People's Republic of China

Y. Zhou
Department of Mechanical and Mechatronics Engineering, Centre for Advanced Material Joining, University of Waterloo, 200 University Ave. West, Waterloo, Ontario N2L 3G1, Canada

W. W. Duley
Department of Physics and Astronomy, University of Waterloo, 200 University Ave. West, Waterloo, Ontario N2L 3G1, Canada

(Received 22 November 2011; accepted for publication 29 February 2012; published 16 July 2012)

Nanojoining, a burgeoning research area, becomes a key manufacturing of complicated nanodevices with functional prefabricated components. In this work, various nanojoining methods are first reviewed. For nanojoining of Ag/Au nanoparticles, three methods are investigated comparatively. Thermal annealing shows a two-step solid state diffusion mechanism. Laser annealing by millisecond pulses displays the thermal activated solid state diffusion. Meanwhile, two effects have been identified in femtosecond laser irradiation with different laser intensities: photofragmentation at rather high intensity ($\sim 10^{14}$ W/cm^2) and nanojoining at low intensity ($\sim 10^{10}$ W/cm^2). The photofragmentation forms a large number of tiny nanoparticles with an average size of 10 nm. Control over irradiation conditions at intensities near 10^{10} W/cm^2 results in nanojoining of most of the nanoparticles. This nanojoining is obtained through a nonthermal melting and a surface fusion welding. Joined Au nanoparticles are expected to have numerous applications, such as probes for surface enhance Raman spectroscopy. © *2012 Laser Institute of America*.

Key words: femtosecond laser, nanowelding, plasmonics

I. INTRODUCTION

Joining (welding, brazing, soldering, bonding, etc.), whether at macro-, micro-, or nanoscales, is an essential step of man-made product manufacturing and assembly, providing mechanical support and integration, electrical connection, optical coupling, environmental protection, etc.[1] Nanojoining is one kind of bottom-up nanofabrications which enables the direct assembly of low-dimensional nanostructures for nanodevices.[2–7] It is important to point out that there is an emerging need to join nanoscale building blocks, such as nanoparticles (NPs) and nanowires, to themselves and/or dissimilar nanocomponents and/or molecular-components to form functional nanodevices and systems, and then to join these to the surroundings, to be integrated into micro- and macro-scale devices and systems.[2–7] Otherwise, industrial scale production of these nanoscale devices is not possible, as experienced both at macro- and micro-scales. As devices become increasingly smaller, challenges faced in micro- and nanojoining must be overcome before these joints are safely implemented. For examples, a proper manipulation of nanoscaled building blocks has to be developed during assembly. For fusion welding, researchers must determine how to robustly join these miniature building blocks while avoiding excessive damage. When the building blocks shrink into submicro or even to a range of nanometers, such as the fabrication of nanomechanical engineering systems (NEMS), the melting has to be controlled within a thickness of few nanometers. Ultrafast pulsed laser is an innovative tool in this field for nanoscopic processing.[6,7] Femtosecond laser irradiation can result in an ultrafast and nonthermal melting of solid materials, which is promising for developing novel joining technologies for nanodevices and/or molecular devices. With the development of nanoscience and nanotechnology, nanoscopic joining technologies are finding more and more applications. However, a comparative study between thermal nanowelding and nonthermal nanowelding induced variable laser pulse widths is still rare. Such a systematic investigation is of benefits to elucidating the features of various nanoweldings suitable for a certain application.

In this paper, we first reviewed various nanojoining methods. Subsequently, we presented three methods to join Au/Ag nanoparticles. Thermal sintering, laser annealing with millisecond laser pulses, and femtosecond laser induced welding were compared. Different joining mechanisms were elucidated. These results could be guidelines for developing proper nanojoining strategies for practical devices.

II. NANOJOINING MINIREVIEW

Table I displays the classifications of recent progresses of various nanojoining methods. Although the current review is not listed in a chronological order, we will start with the nanojoining of carbon nanotubes (CNTs) since the development of nanojoining is initially driven by huge amounts of studies on the characterization and application of carbon nanotubes. Gong *et al.* developed a mechanical clamping method using carbon nanotube films to wrap the carbon nanotube strands.[8] Both strong mechanical joining and electrical interconnection are achieved. Yung *et al.* used two carbon nanotube arrays to realize the flip chip packaging.[9] The interwall von der Waals interaction provides robust mechanical joining and electrical contacts. Dong and Arai displayed a concept of nanotube bearing using multiwall carbon nanotubes.[10] The surface clamping between the different layers of nanotubes is employed. These joining methods are sorted to *mechanical joining*.

Adhesive bonding, suitable for joining at different levels: regular to micro- and nanoscales, uses an organic substance (adhesive) to join two parts together. Similar to soldering/brazing, liquid adhesive needs to be able to wet the surfaces of the building blocks so that the free energy of the system associated with the original surfaces is reduced.[1] Gu *et al.*[11] has used adhesives to join multisegmented Au-Ni-Au rods of 150–250 nm diameter and 2–6 μm length into two- or three-dimensional structures/networks. To improve the tensile properties of carbon nanotube strands, epoxy resin was intercalated into nanotube bundles.[12] Such a composite can be mechanically joined to other materials, although electrical contacts need to be solved. Recently, a so-called "plasmonic ruler" is developed by coupling metallic nanoparticles with DNA molecules or peptides.[13,14] Since a light-scattering spectrum strongly depends on the gap, a nanoscale distance can be measured by such a device based on the surface plasmonic resonance.

Solid state bonding includes diffusion nanobonding, ultrasonic welding, and electron beam bonding. Diffusion nanobonding using metallic nanoparticles as bond layers is a popular nanojoining process currently under study. In this solid state nanobonding process, nanoparticles are sintered to form networks, and at the same time, these networks are joined to substrates, all assisted by diffusion with driving force to reduce surface areas. As the size of nanoparticles reduces, diffusion is enhanced because of lower activation energy and increased specific surface energy, which can result in the decrease of sintering and bonding temperature.[5,15,16] This is important since there is increasing interest in the development of low temperature joining processes for polymeric based microelectronics applications.[6] *Ultrasonic nanowelding* has been developed to join CNTs to Ti electrodes[17] for the development of carbon nanotube-based photovoltaic cells with high energy conversion efficiency.[18] Low Ohmic contact has been achieved between the Ti electrodes and the CNTs because of the formation of covalent C-Ti bonds, which is in fact the mechanism responsible for joining.[19] *Cold nanowelding* has been used to join ultrathin single-crystal Au nanowires using only mechanical contact at close to room temperature in a high-resolution transmission electron microscope (TEM) equipped with scanning tunneling microscope (STM).[2] The electron beam is directed to induce structural defects, "vacancies" and "interstitials," at the crossing point of two CNTs. Self rearrangement of those affected carbon atoms occurs at high specimen temperature (800 °C in Ref. 4) so as to form heptagonal or octagonal rings, thus producing internanotube junctions. The lowering of energy of the system is obviously the driving force to form the junctions, confirmed by molecular dynamics simulation.

Recently *nanosoldering* has drawn significant attention as a possibly significant joining process in the assembly and integration of nanoelectronics devices. Girit and Zettl[20] used a micromanipulator with a tungsten tip to solder In-Tin alloy to make an Ohmic contact on graphene, a single atomic layer of carbon. With a nanomanipulator within a scanning electron microscopy (SEM), Peng *et al.* joined Au to Pt-Co nanowires with SnAu nanowires as solders melted by Joule heating.[3] This kind of process, where only a single weld is made, can be slow and costly because of the requirements for accurate manipulation of the parts and the execution of the joining operation. As an attractive alternative, batch operation allows multiple joints made at the same time. This is illustrated in the following example on reflow soldering of multisegmented metal nanowires.[11,21] Multisegmented metal (such as Sn/Au/Ni) nanowires were fabricated using an electrodeposition method in nanoporous templates. In one example, Tin was grown on the ends of Au nanowires with Ni/Au as under-layers (Ni as a diffusion barrier and Au as wetting layer) and then the Sn/Au/Ni coated Au nanowires were reflow soldered together in a liquid medium. A magnetic field was also employed to align the nanowires to form three-dimensional nanowire networks. Mafuńe *et al.*[22] used nanosecond pulsed laser to melt Au nanoparticles to braze Pt nanoparticles together to form three-dimensional networks. Wu *et al.*[19] have brazed CNT bundles to Ni electrodes with Ag-Cu-Ti alloy under vacuum of 10^{-6} Torr. XPS analysis revealed the brazing mechanism as the formation of Ti-C covalent bonds, similar to what happened in ultrasonic welding of CNTs to Ti electrodes.[17,18] It is well known that an

TABLE I. Classification of typical nanojoining processes.

Conventional catalog	Nanojoining
Mechanical joining	Mechanical clamping
	Von der Waals force (Refs. 8–10)
Adhesive joining	CNT/epoxy, polymer (Refs. 11 and 12),
	DNA or peptide (Refs. 13 and 14)
Solid state bonding	Electron beam (Ref. 4)
	Diffusion bonding/sintering/cold welding (Refs. 2, 6, 15, and 16)
	Ultrasonic welding (Refs. 17 and 18)
Soldering/brazing	Liquid-phase reflow soldering (Refs. 11 and 21)
	Resistance soldering (Ref. 3)
	Active brazing (Ref. 19)
	Laser brazing (Ref. 22)
Fusion welding	Resistance (Refs. 24 and 25)
	Ultrafast laser (Refs. 6 and 7)

active alloying element, such as Ti, is needed so that the molten braze or solder will be able to wet on ceramics in so-called the active brazing/soldering.[1] The joint strength displayed a maximum around 900–950 °C because at higher temperatures CNTs started to degrade due to their reaction with the brazing materials and catalytic compounds. With the brazed CNT bundles, an incandescent lamp filament can be fabricated with high light emission efficiency due to the much lower contact resistance enabled by active brazing.[23]

Fusion nanowelding processes have been attempted with various heat sources, such as laser beam,[5,22] Joule heating[24,25] similar to that used in resistance welding,[1] and even a resistively heated hot stage.[26] The joint is formed by resolidification (fusion) of the molten metal at the faying surfaces produced by Joule heating. The voltage across the junction reduces slightly once the weld forms and then stays unchanged, indicating an Ohmic contact has been formed. This resistance nanowelding approach has also been used to join dissimilar metals, e.g., Pt nanowire to thin Au wire to produce heterojunctions.[24] A hot stage within a SEM has been used to weld two crossed semiconductor Ge nanowires coated with thin layers of carbon sheath.[26] This localized welding is possible due to the porous nature of the carbon sheath, which allows the molten Ge to fuse together and later solidify at the contact point.

Nonthermal nanowelding by ultrashort laser pulse (shorter than picoseconds) is reviewed here as conceptually separated from other fusion nanowelding processes since the nature of interaction between ultrafast laser pulses and materials is known as nonthermal processing.[27] As the electron-lattice thermal coupling time (typical a few picoseconds) is much longer than the laser pulse width, the electrons do not have enough time to transfer energy to the lattice. At a fluence larger than the surface damage threshold,[27] electrons are excited, ejected, and thereby weaken the chemical bonds of lattice atoms, resulting in "melting" of surface atoms, which is a nonthermal phenomenon.[5,27–29] This melting also occurs only on the surface to a nanoscale depth without damaging the bulk and, thus, can be used for welding of nanoparticles.[5]

III. EXPERIMENT

Au NPs were synthesized by reducing $HAuO_4$ with $NaBH_4$ and stabilized by sodium citrate. Ag NP solution was prepared by reducing $AgNO_3$ with sodium citrate. The concentration of nanoparticles was controlled as 1 mM. Au/Ag nanoparticle films were prepared by immersing glass slides or silica wafers into the solution for at least 48 h. The solution-deposited glass slides were used to characterize the optical properties, and Si wafers were employed for microstructure and laser sintering investigations. The deposited films were also fabricated by directly dripping condensed nanoparticles.

Thin films on glass and Si wafer substrates were annealed by various sources: a hot-plate, a Nd:YAG-pulsed laser (Miyachi LW-50A, wavelength = 1064 nm, pulse width = 1 ms, maximum average power = 5 kW, and focused beam size = 0.6 mm) at different laser powers, or a femtosecond laser (100 nm, 0.3 mJ/pulse, 1 KHz). The morphology of the as-synthesized Ag NPs, deposited and annealed Ag NP thin films on glass and Si wafer substrates was characterized by scanning probes microscopy (SPM, Vecco 3100) and scanning electron microscopy (LEO 1530), respectively. TEM samples were synthesized by dripping on Cu grid coated carbon films. TEM observation was carried out with a JOEL 2010F. Absorbance spectra of thin films were measured with UV-vis-near-infrared (NIR) spectroscopy (Shimadzu, UV-2500).

IV. RESULTS AND DISCUSSION

A. Thermal and laser annealing

Figure 1(a) shows the deposited Ag NP films on glass substrates. The average size is about 50 nm. Figure 1(b) shows a typical SPM image of Ag NPs sintering at 573 K for 5 min. The bonding is evident by the forming of the necking connection between Ag NPs. These joints can be attributed to solid state diffusion because these NPs are expected to melt at a temperature ranging from 673 to 873 K based on the size effect,[29] above the present sintering temperature. The blank area without Ag NPs dramatically increases, probably due to the melting and evaporation of tiny nanoparticles. Figure 1(c) presents the effect of laser annealing with a single pulse of energy of 0.12 J. The bridging path occurs in the neighboring Ag NPs, orients arbitrarily, and eventually generates 3D connection network. The temperature is estimated as 573 K at the energy of 0.12 J according to a thermal diffusion model.[30] Figure 1(d) shows the melting of nanoparticles at a pulse energy of 0.2 J, which corresponds to a temperature of 450 °C. The melting of Ag NPs is identified at this stage, which results in the remarkable shape change and coarsening of Ag NPs. Differences between thermal sintering and pulsed laser annealing are also obvious. Although laser annealing also results in a porous structure blank areas is significantly smaller than thermal sintering samples.

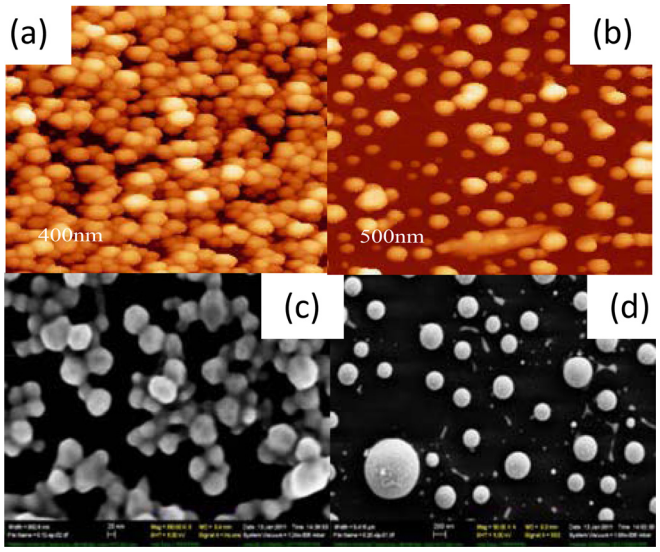

FIG. 1. SPM images of (a) Ag NPs on glass substrates, (b) thermal sintering at 300 °C for 5 min; SEM images of (c) laser annealing at 0.12 J and (d) 0.2 J with a pulse width of 1 ms.

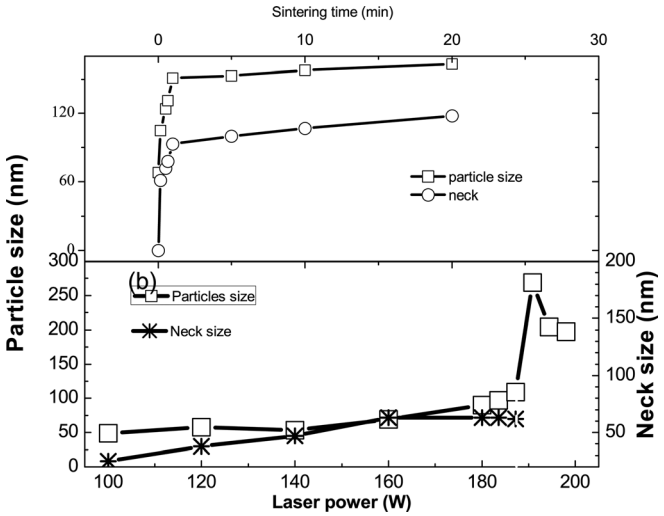

FIG. 2. (a) Neck size and particle diameter as a function of thermal annealing time at 300 °C. (b) Neck size and particle diameter vs laser power for a 1 ms single pulse.

Nanoparticle surface becomes somehow smooth after thermal sintering while the polygon features are more remarkable in laser annealing. It seems that there are much more chain-style structures in thermal sintering. Joint clusters are more arbitrary in laser annealing.

Figure 2 presents the average results of the particle size and the neck size obtained by statistically measuring over 20 particles for the samples (a) thermally annealed at 300 °C for different times and (b) laser annealed with increasing laser powers. It is evident that for thermal sintering the neck grows very fast till 50% of particle size and then increases slowly in thermal sintering. Meanwhile, Ag nanoparticles dramatically coalesce once the initial fast neck growth completes. These results are consistent with Monte Carlo simulation and can be explained by the surface energy driven solid state diffusion.[5,15] For laser annealing, the neck size displays a proximately linear increase with the laser power. In contrast, the particle size during laser annealing almost keeps constant till it starts melting. Further increasing laser power beyond the melt at the threshold power leads the decrease of the particle size due to the evaporation. These results can be explained by different annealing rates/periods. For thermal sintering, the heat rate is quite slow (about 1–10 °C/min). There is enough time for the mass transfer through surface diffusion between two nanoparticles. This results in the solid state diffusion and the coalescence of nanoparticles. However, the heat rate of pulse laser annealing is a few orders higher than a conventional heating rate. The theoretical estimation that this rate can be 4×10^5 °C/s. Although the bonding can be formed due to the surface diffusion but this diffusion gets weaker or even stops immediately after laser irradiation. This hinders the further coalescence of nanoparticles.

Previous studies on the sintering of Ag nanoparticles elucidate that the dense structure can be obtained by suppression of low temperature surface diffusion while enhancing the lattice/grain-boundary diffusion.[31,32] It is well known that the lattice diffusion occurs at a higher temperature than surface diffusion although there is no clear temperature point to separate two diffusions. Obviously, a higher heating rate will facilitate the lattice and/or grain-boundary diffusion and result in a denser structure. Keeping this in mind, it is natural to think that a liquid sintering is of more benefits for a dense structure. This is the reason why we consider a nonthermal welding with femtosecond laser irradiation.

B. Femtosecond laser nonthermal nanowelding

Figures 3(a) and 3(b) show the 1 mM Au nanoparticle solution before and after irradiated at a laser intensity of 4×10^{14} W/cm^2 for 10 min. As-grown Au nanoparticles (before irradiation) have an average size of 15 nm. Two effects have been observed by femtosecond laser irradiation: the generation of large number of tiny nanoparticles with a size of 1–3 nm; welding of 2–3 Au nanoparticles with a size around 15 nm. It is reasonable to deduce that these tiny nanoparticles are created by the fragmentation of Au nanoparticles through laser irradiation. A previous study has identified the electron ejection as the first step of photofragmentation by nanosecond laser pulses.[33] This electron emission causes nanoparticles to become positively charged, and the repulsion among the charges leads to fragmentation. Compared to nanosecond laser, the interaction between femtosecond laser pulses and matter is dominant by electron ejections and there is little energy transferring between excited Au electrons and Au lattice.[34] It is, thus, expected that the effective photofragmentation will occur in femtosecond laser irradiation. The laser induced breakdown of water occurs at the intensity of around 10^{12} W/cm^2 in case of the pulse width of 100 fs.[35] At present experiments, about 5 mm long filamentary area is found in Au nanoparticle solution in the vicinity of the focal point. This indicates that water is broken by the focused laser in the regime. It is possible that rich ions from water breakout and vibrated filaments of

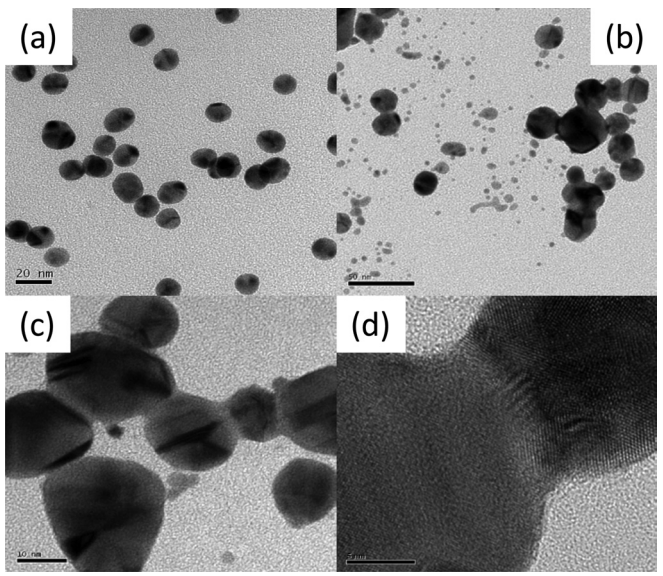

FIG. 3. Nanowelded Au nanoparticles by femtosecond laser irradiation. (a) Pristine liquid, (b) irradiation at a intensity of 4×10^{14} W/cm^2, (c) irradiation at 3×10^{10} W/cm^2, and (d) local structures of typical welded necks between two particles shown in (c). Note that the scales are 20 nm in (a), 50 nm in (b), 10 nm in (c) and 5 nm in (d).

extremely intensive laser enhance the fragment of Au nanoparticles. This is evident in Fig. 3(c) where only welded Au nanoparticles are observed. Besides, it is worth noting that heating–melting–evaporation processes are also observed in nanosecond laser irradiation.[36] It is difficult to attribute such a thermal mechanism for the welding of Au nanoparticles since the thermal coupling time between electrons and lattice is about 1 ps, remarkably longer than the laser pulses. Besides, the nanoparticles in Fig. 3(d) keep polycrystalline indicating a nonthermal welding mechanism by femtosecond laser irradiation. Compared to thermal sintering and millisecond laser annealing shown in Fig. 1, joined nanoparticles are still well kept their original shapes, indicating only surface melting. High-resolution TEM shown in Fig. 3(d) clearly shows that two Au nanoparticles are welded with metallic bonds.

Figure 4 shows the thermal effect of different heating mechanisms on nanoparticles. For a nanosecond laser pulses or even longer pulses (the thermal sintering is equal to the annealing by a continuing wave laser), the thermal effect is dominant, i.e., the whole nanoparticle will be heated. At a threshold temperature, nanoparticles will melt and change their shape. Meanwhile, for a fs pulse, only the surface lattice will be heated because the laser pulse width is much shorter than the characteristic time of the thermal diffusion.[28] The surface melting will be the significant feature of fs laser irradiation. This melting is due to the lattice bonding softening associated with electron excitation and ejection. Because this surface melting occurs at a nanoscale[5] the shape and size of nanoparticles will be kept roughly unchanged. Such phenomena have been evident in Figs. 4(c) and 4(d).

C. Plasmonic properties of welded nanoparticles

Plasmonic properties of welded Ag nanoparticles are numerically simulated by 3D finite element method with the Drude–Lorentz model.[37,38] The complex permittivity of the silver is using experimental data. Figure 5 shows comparative electrical potential distributions between two and four adjacent and welded nanoparticles in air. The diameter of the nanoparticle is 50 nm, and the gap is 5 nm for adjacent pair and −5 nm for welded pair (i.e., the overlapped central distance is 5 nm). The results displays that welded nanoparticles possess a

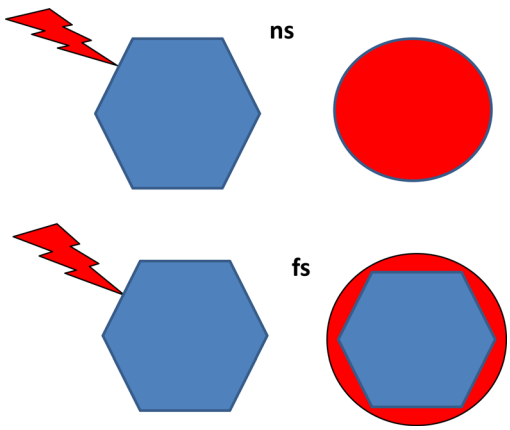

FIG. 4. Thermal effect of nanoparticles by laser irradiation with nanosecond and femtosecond pulse widths.

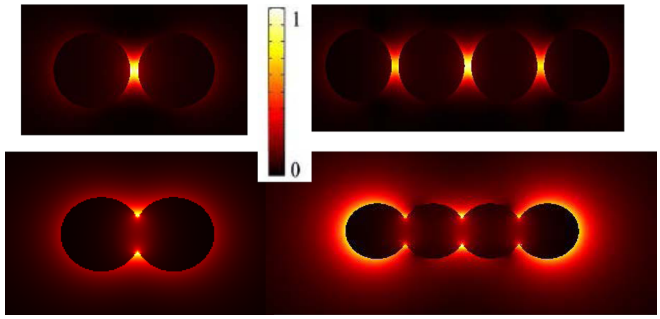

FIG. 5. The cross-sectional views of normalized electric field distributed at the surface of the nanostructures in air, top panels: adjacent two and four Ag spheres with a diameter of 50 nm and a central gap of 5 nm; low panels: welded two and four Ag spheres at the same diameter and a overlapped central distance of 5 nm (i.e., the central gap of −5 nm).

ring-shape hot spot in the neck area compared to a central point in simply adjacent nanoparticle pairs. This clearly indicates an increasing area of hot-spots. Besides, unlike adjacent dimmers or trimmers which are bonded by weak interaction, welded nanoparticles form strong and permanent joins, which can work as stable Raman probes for repeatable analysis.

Figure 6 presents the surface enhanced Raman spectra (SERS) of adenine at a concentration of 10^{-4} M with different probes. There are only very weak features with silver foil. However, enhanced SERS spectrum is evident with Ag nanoparticles before joining. After joining, these Raman features are further enhanced to 5–6 times by comparison to Ag nanoparticles, especially 1040, 1160, 1230, 1380, 1440 cm^{-1} are clearly identified. Strong C5N5 ring vibration modes are identified at 730 and 1320 cm^{-1}.

Various interactions between femtosecond laser pulses and matter can be summarized in Fig. 7. With intense pulse energy, the focusing beam can create a crater on the sample surface. On the bottom of crater, the material will experience a shock-wave processing. Compressive lattice could be frozen at a metastable stressed state and result in enhanced mechanical hardness. With lower pulse energy, one can carry out micromachining and/or nanomachining. Our results

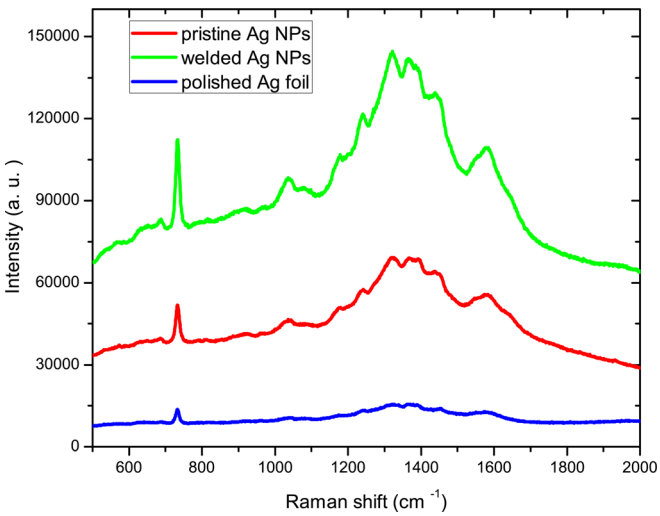

FIG. 6. Enhanced Raman spectroscopy of adenine with a concentration of 10^{-4} M with different SERS probes.

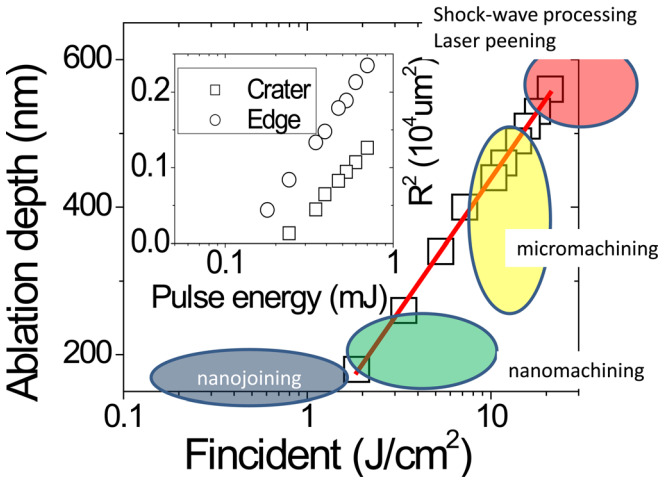

FIG. 7. Various interactions between femtosecond laser and materials. The data are adapted from our previous study on the irradiation of graphite with 120 fs laser pulses (Ref. 5).

show femtosecond laser pulses can create very steep ablated groove and nanopatterning with precisely control pulse energy. Nanojoining occurs at an even lower fluence, which is around 10^{10} W/cm^2 for Ag nanoparticle processing. It is worth noting that at a fluence lower than the surface damage threshold, the incident femtosecond laser will be simply reflected.[27] There is no surface melting occurring, and thereby, the surface damaged threshold is the lower limit fluence for nanojoining. By scanning the surface, it is not challenged to generate nanowelded films in a large area. Such a large film with tunable plasmonic properties is promising for solar photovoltaics and opto-electronic application.[38–40]

V. CONCLUSIONS

Nanojoining, as a flexible manufacturing approach become an increasing significant nanofabrication of hybrid nanodevices. We provide a brief review of recent progresses in this field and latest results in the Center of Advance Material Joining, University of Waterloo. We compare three annealing mechanisms for nanojoining, namely, thermal sintering, millisecond laser annealing, and femtosecond laser irradiation. Femtosecond laser irradiation displays a nonthermal welding mechanism which is promising to build complex nanodevices without modifying the central structures of nanoscopic building blocks. We displays that welded Au nanoparticles can work as effective Raman probes for surface enhanced Raman spectroscopy.

ACKNOWLEDGMENTS

This work is partially supported by Canadian Research Chair program and NSERC discovery grant. Z. X. Zhang would like to thank NSFC-Research Fund for International Young Scientists No. 60910187, Ministry of Education, People's Republic of China.

[1]Y. Zhou, *Microjoining and Nanojoining* (Woodhead Publishing Ltd, Cambridge, England, 2008).
[2]Y. Lu, J. Huang, C. Wang, S. Sun, and J. Lou, "Cold welding of ultrathin gold nanowires," Nat. Nanotechnol. **5**, 218–224 (2010).
[3]Y. Peng, T. Cullis, and B. Inkson, "Bottom-up nanoconstruction by the welding of individual metallic nanoobjects using nanoscale solder," Nano Lett. **9**, 91–96 (2009).
[4]M. Terrones, F. Banhart, N. Brobert, J. C. Charlier, H. Terrones, and P. M. Ayayan, "Molecular junctions by joining single-walled carbon nanotubes," Phys. Rev. Lett. **89**, 075505–1–4 (2002).
[5]A. Hu, M. Rybachuk, Q.-B. Lu, and W. W. Duley, "Direct Synthesis of sp-bonded carbon chains on graphite surface by femtosecond laser irradiation," Appl. Phys. Lett. **91**, 1319061–1–3 (2007).
[6]A. Hu, J. Y. Guo, H. Alarif, G. Patane, Y. Zhou, G. Compagnini, and C. X. Xu, "Low Temperature sintering of Ag nanoparticles for flexible electronics packaging," Appl. Phys. Lett. **97**, 153117–1–3 (2010).
[7] S. J. Kim and D. J. Jang, "Laser-indiced nanowelding of gold nanoparticels," Appl. Phys. Lett. **86**, 033112–1–3 (2005).
[8]T. Gong, Y. Zhang, W. Liu, J. Wei, C. Li, K. Wang, D. Wu, and M. Zhong, "Connection of macro-sized double-walled carbon nanotubes strands by bandaging with double-walled carbon nanotube films," Carbon **45**, 2235–2240 (2007).
[9]K. P. Yung, J. Wei, and B. K. Tay, "Formation and assembly of carbon nanotube bumps for interconnection applications," Diamond Relat. Mater. **18**, 1109–1113 (2009).
[10]L. Dong and F. Arai, "Destructive Constructions of nanostructures with carbon nanotubes through nanorobotic manipulation," IEEE/ASME Trans. Mechatron. **9**, 350–357 (2004).
[11]Z. Gu, H. Ye, D. Smirnova. D. Small, and D. H. Gracias, "Reflow and electrical characteristics of nanoscale solder," Small **2**, 225–229 (2006).
[12]Y. Li, K. Wang, J. Wei, Z. Gu, Q. Shu, C. Li, W. Wang, Z. Wang, J. Luo, and D. Wu, "Improving tensile properties of double-walled carbon nanotube strands by intercalation of epoxy resin," Carbon **44**, 176–179 (2006).
[13]N. Liu, M. Hentschel, T. Weiss, A. Paul Alivisatos, and H. Giessen, "Three-dimensional plasmon rulers," Science **332**, 1407 (2011).
[14]C. Sonnichsen, B. M. Reinhard, J. Liphardt, and A. P. Alivisatos, "A molecular ruler based on plasmon coupling of single gold and silver nanoparticles," Nat. Biotechnol. **23**, 741–745 (2005).
[15]H. Alarifi, A. Hu, M. Yavuz, and Y. Zhou, "Silver nanoparticle paste for low-temperature bonding of copper," J. Electron. Mater. **40**, 1394–1342 (2011).
[16]E. Ide, S. Angata, A. Hirose, and K. F. Kobayashi, "Metal-metal bonding process using Ag metallo-organic nanoparticles," Acta Mater. **53**, 2385–2393 (2005).
[17]C. Chen, Y. Lu, E. S. Kong, Y. F. Zhang, and S. T. Lee, "Nanowelded carbon-nanotube-based solar microcells," Small **4**, 1313–1318 (2007).
[18]C. Chen, L. J. Yan, E. S. Kong, and Y. F. Zhang, "Ultrasonic nanowelding of carbon nanotubes to metal electrodes," Nanotechnology **17**, 2192–2197 (2006).
[19]W. Wu, A. Hu, X. Li, J. Wei, Q. Shu, K. Wang, M. Yavuz, and Y. Zhou, "Vacuum brazing of carbon nanotube bundles," Mater. Lett. **62**, 4486–4488 (2008).
[20]C. O. Girit and A. Zettl, "Soldering to a single atomic layer," Appl. Phys. Lett. **91**, 193512–1–3 (2007).
[21]F. Gao, S. Mukherjee, Q. Cui, and Z. Gu, "Synthesis, characterization, and thermal properties of nanoscale lead-free solders on multisegamented metal nanowires," J. Phys. Chem. C **113**, 9546–9552 (2009).
[22]F. Mafuńe, J. Kohno, Y. Takeda, and T. Kondow, "Nanoscale soldering of metal nanoparticles for construction of higher-order structures," J. Am. Chem. Soc. **125**, 1686–1687 (2003).
[23]Y. Zhou, A. Hu, M. I. Khan, W. Wu, B. Tam, and M. Yavuz. "Recent progress in micro and nano-joining," J. Phys. Conf. Ser. **165**, 012012–1–6 (2009).
[24]H. Tohmyoh, T. Imazumi, H. Hayashi, and M. Saka, "Welding of Pt nanowires by Joule heating," Scr. Mater. **57**, 953–956 (2007).
[25]H. Tohmyoh and S. Fukui, "Self-completed Joule heat welding of ultrathin Pt wires," Phys. Rev. B **80**, 155403–1–7 (2009).
[26]Y. Wu and P. Yang, "Melting and welding of semiconductor nanowires in nanotubes," Adv. Mater. **13**, 520–523 (2001).
[27]D. H. Reitze, H. Ahn, and M. C. Downer, "Optical properties of liquid carbon measured by femtosecond spectroscopy," Phys. Rev. B **45**, 2677–2693 (1992).
[28]D. Von der Linde, K. Sokolowski-Tinten, and J. Biakowski, "Laser-solid interaction in the femtosecond time regime," Appl. Surf. Sci. **109/110**, 1–10 (1997).
[29]A. Hu, Y. Zhou, and W. W. Duley, "Femtosecond laser-induced nanowelding: Fundamentals and applications," Open Surf. Sci. J **3**, 42–49 (2011).

[30]K. Dick, T. Dhanasekaren, Z. Zhang, and D. Meisel, "Size-dependent metling of silica-encapsulated gold nanoparticles," J. Am. Chem. Soc. **124**, 2312–2317 (2002).
[31]P. Peng, A. Hu, and Y. Zhou, "Laser sintering of silver nanoparticle thin films: Microstructure and optical properties," Appl. Phys. A (to be published).
[32]J. G. Bai, T. G. Lei, J. N. Calata, and G. Q. Lu, "Control of nanosilver sintering attained through organic bonder burnout," J. Mater. Res. **22**, 3494–3500 (2007).
[33]T. G. Lei, J. N. Calata, G. Q. Lu, X. Chen, and S. Luo, "Low-temperature sintering of nanoscale silver paste for attaing large-area chips," IEEE Trans. Compon. Packag. Technol. **33**, 98–104 (2010).
[34]A. Hu, J. Sanderson, A. A. Zaidi, C. Wang, T. Zhang, Y. Zhou, and W. W. Duley, "Direct synthesis of polyyne molecules in acetone by dissociation using femtosecond laser irradiation," Carbon **46**, 1792–1828 (2008).
[35]A. Hu, S. K. Panda, M. I. Khan, and Y. Zhou, "Laser welding, microwelding, nanowelding and nanoprocessing," Chin. J. Lasers **36**, 3149–3159 (2009).
[36]P. K. Kennedy, D. X. Hammer, and B. A. Rockwell, "Laser-induced breakdown in aqueous media," Prog. Quantum. Electron. **21**, 155 (1997).
[37]S. Nolte, C. Momma, H. Jacobs, A. Tunnermann, B. N. Chichkov, B. Wellegehausen, and H. Welling, "Ablation of metals by ultrashort laser pulses," J. Opt. Soc. Am. B **14**, 2716–2722 (1997).
[38]T. Zhang, X. Y. Zhang, X. Xue, X. Wu, C. Li, and A. Hu, "Plasmonic properties of welded metal nanoparticles," Open Surf. Sci. J. **3**, 76–81 (2011).
[39]X. Y. Zhang, A. Hu, T. Zhang, W. Lei, X. J. Xue, Y. Zhou, and W. W. Duley, "Self-assembly of large-scale and ultrathin silver nanoplate films with tunable plasmon resonance properties," ACS Nano **5**, 9082–9092 (2011).
[40]H. Wu, L. Hu, M. W. Rowell, D. Kong, J. J. Cha, J. R. McDonough, J. Zhu, Y. Yang, M. D. McGehee, and Y. Cui, "Electrospun metal nanofiber webs as high-performance transparent electrode," Nano Lett. **10**, 4242–4248 (2010).